Analysis of Coherence in Global Seismic Noise for 1997–2012

A. A. Lyubushin

Schmidt Institute of Physics of the Earth, Russian Academy of Sciences,
ul. Bol'shaya Gruzinskaya 10, Moscow, 123995 Russia
e-mail: lyubushin@yandex.ru

Abstract—The coherent behavior of four parameters characterizing the global field of low-frequency (periods from 2 to 500 min) seismic noise is studied. These parameters include logarithmic variance, kurtosis (coefficient of excess), width of support of multifractal singularity spectrum, and minimal normalized entropy of the distribution of the squared orthogonal wavelet coefficients. The analy)sis is based on the data from 229 broadband stations of GSN, GEOSCOPE, and GEOFON networks for a 16-year period from the beginning of 1997 to the end of 2012. The entire set of stations is subdivided into eight groups, which, taken together, provide full coverage of the Earth. The daily median values of the studied noise parameters are calculated in each group. This procedure yields four 8-dimensional time series with a time step of 1 day with a length of 5844 samples in each scalar component. For each of the four 8-dimensional time series, the frequency-time diagram of the evolution of the spectral measure of coherence (based on canonical coherences) is constructed in the moving time window with a length of 365 days. Besides, for each parameter, the maximum-frequency values of the coherence measure and their mean over the four analyzed noise parameters are calculated as a measure of synchronization that depends on time only. Based on the conducted analysis, it is concluded that the increase in the intensity of the strongest ($M \geq 8.5$) earthquakes after the mega-earthquake on Sumatra on December 26, 2004 was preceded by the enhancement of synchronization between the parameters of global seismic noise over the entire time interval of observations since the beginning of 1997. This synchronization continues growing up to the end of the studied period (2012), which can be interpreted as a probable precursor of the further increase in the intensity of the strongest earthquakes all over the world.

INTRODUCTION

Study of the characteristics of noise in complex (including nonlinear) systems is one of the most promising directions of scientific research. Such studies lie at the borderline of different disciplines since there is much more similitude in this field than the differences associated with the individual properties of the studied objects. In this sense, the study of such a complex system as the Earth constitutes no exception. The low-frequency seismic noise caused by the interaction between the lithosphere, atmosphere, and ocean has a complicated statistical structure, which contains the information about the preparation of the geological catastrophes including large earthquakes. The correlation between the low-frequency microseisms and the intensity of ocean waves is thoroughly studied in (Berger, Davis, and Ekstrom, 2004; Kobayashi and Nishida, 1998; Rhie and Romanowicz, 2004; Tanimoto, 2005). The Earth's crust is the propagation medium for energy from atmospheric and oceanic processes and, since the transfer properties of the crust depend on its state, the statistical characteristics of the microseisms reflect the variations in the parameters of the lithosphere parameters. Various prognostic properties of the low-frequency seismic noise before the strongest earthquakes including mega-earthquakes on Sumatra on December 26, 2004

and in Japan on March 11, 2011 are explored in (Sobolev, 2004; 2008; 2011; Sobolev, Lyubushin, and Zakrzhevskaya, 2005; 2008; Sobolev and Lyubushin, 2006; 2007; Lyubushin and Sobolev, 2006; Lyubushin, 2007; 2008; 2009; 2010; 2011b; 2012a; 2012b; 2013a; 2013b). These studies are based on the data from a few (at most 10) stations of the global seismic networks or broadband seismic measurements by the national F-net network in Japan.

In this paper, the analysis covers the data from a large number of broadband seismic stations globally distributed all over the world. Such an analysis was previously conducted in (Lyubushin, 2013b) with the purpose to reveal the areas of the strongest linear synchronization between the parameters of seismic noise. The aim of the present study is to identify the global effects of synchronization in seismic noise in a moving time window for the interval of 1997 to 2012. It is known that, starting from the mega-earthquake on Sumatra on December 26, 2004, the Earth experienced a series of strongest earthquakes ($M \geq 8.5$), which have not occurred since the beginning of 1965. Thus, the last ten years are marked by the significant enhancement of seismicity. The following questions now arise: how is this activation reflected in the coherence of time series of the parameters characterizing the global seismic noise? Had such synchronization
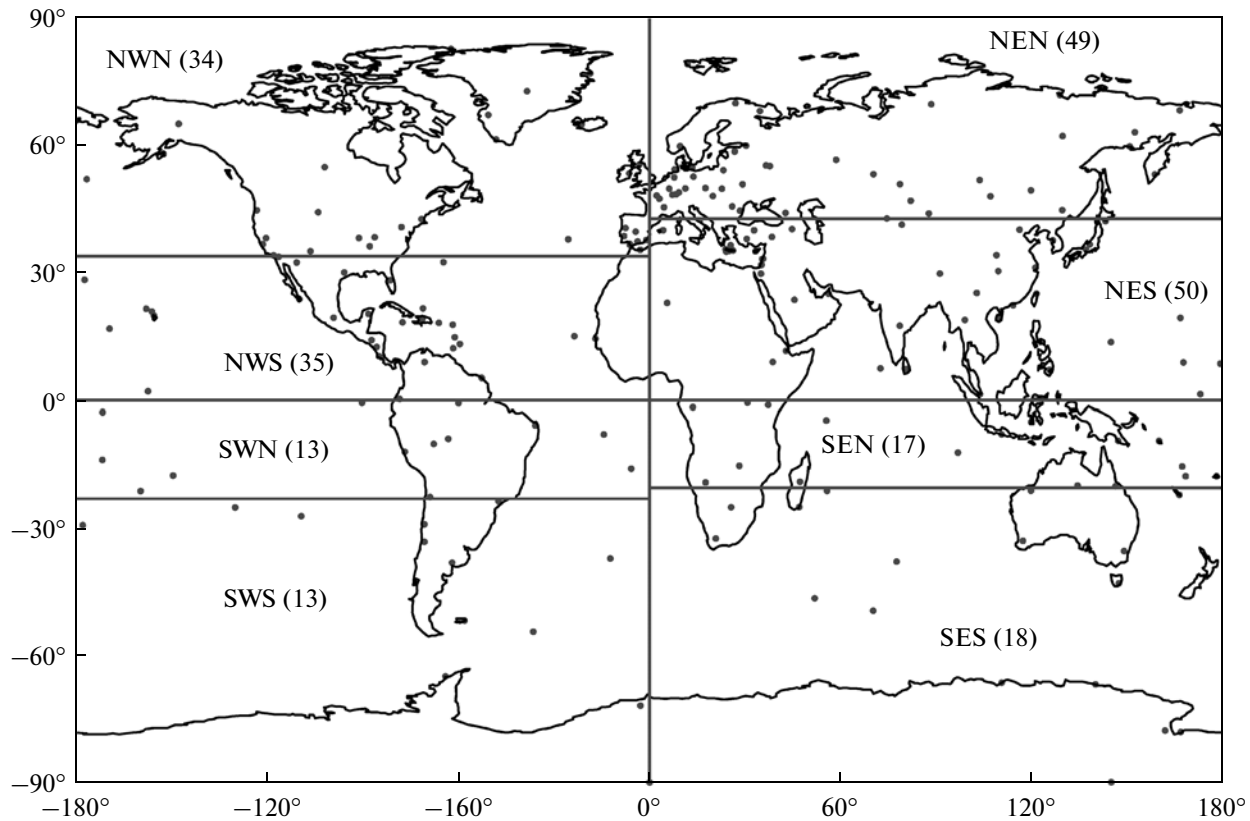
Fig. 1. The layout of 229 broadband seismic stations of a cluster of three global seismic networks and their subdivision into eight groups. The number of the stations in the group is indicated in the brackets after the name of the group.

been present in the seismicity before the end of 2004? And, therefore, can these effects of noise synchronization be considered as a precursor of the observed burst of seismicity in the Earth? The present paper strives to answer these questions.

THE DATA

The progress in observational seismology has brought a unique tool for retrieving the information about the processes in the Earth—the IRIS global seismic network, which was arranged in the end of the 1990s. The continuous data recorded by the standard seismic instruments at different national networks are gathered into a common database and can be then requested and downloaded via Internet by any interested user. This study is based on the digital waveforms of seismic noise that can be requested from IRIS database at http://www.iris.edu/forms/webrequest. The records by the wideband seismic stations from the group of three global seismic networks (Global Seismographic Network, http://www.iris.edu/mda/_GSN; GEOSCOPE, http://www.iris.edu/mda/G; and GEOFON, http://www.iris.edu/mda/GE) are used. The vertical components sampled at 1 Hz (LHZ records) for the 16-year interval from January 1, 1997

to December 31, 2012 downloaded from the database were decimated to the sampling interval of 1 min by calculating the average values on the successive intervals containing 60 counts.

Figure 1 illustrates the layout of 229 broadband stations whose data were used for analyzing the properties of seismic noise. The whole set of the stations is subdivided into eight groups, which are also shown in Fig. 1. The number of the stations in each group is indicated. The names of the groups are formed of the letters N, S, and E standing for North, South, and East. For example, NES means the group of the stations that are located in the northern (N) hemisphere, have eastern longitudes (E), and fall in the southern (S) segment. The stations were grouped by the following principle. First, the stations were classified by their position in the northern or southern hemisphere and then subdivided into the eastern and western parts according to the sign of their geographical latitudes. This procedure yielded four groups (NW, NE, SW, and SE). Then, each of these groups was subdivided by a latitudinal boundary into the northern and southern subgroups in such a way that approximately an equal number of seismic stations fell in each subgroup.

THE STATISTICS OF THE SEISMIC NOISE WAVEFORMS USED IN THE ANALYSIS

Logarithmic Variance and Kurtosis

The simplest statistics for analyzing the seismic noise are variance *Var* and kurtosis (coefficient of excess) κ:

$$Var = \langle (\Delta x)^2 \rangle, \quad \kappa = \langle (\Delta x)^4 \rangle \big/ \langle (\Delta x)^2 \rangle^2 - 3. \qquad (1)$$

Here, Δx are deviations of the seismic noise waveforms from the trend, and the angular brackets denote the operation of time averaging. Statistics (1) were calculated in the successive time windows (without overlapping), which contained 1440 neighboring minute values, which makes up one day. Before calculating statistics (1), independently in each daily window, the data were detrended by a polynomial of degree 8. This procedure eliminates the deterministic trends caused by the influence of tidal and thermal deformations of the Earth's crust and yields the pure data for analyzing the noise. Thus, the time series of *Var* and κ with a sampling interval of one day were obtained for each station. Figure 2a shows the graphs of the daily median values for the variance log(*Var*) calculated for each of the eight groups of stations in Fig. 1. The procedure of taking the median implements averaging over all stations of a group and is robust to the outliers (extreme values), which are quite common in the time series of variance. Due to this, the further analysis is carried out for the medians of log variances.

The kurtosis κ is a measure of the deviation of the distribution of quantity Δx from Gaussian distribution, for which $\kappa = 0$ (Vadzinskii, 2001). Formally, kurtosis can be negative $\kappa < 0$; however, the values of κ for the time series of low-frequency seismic noise analyzed in the present work are mostly positive and, in many cases, even far above unity. Therefore, for better visualization, the median values of kurtosis over the groups of stations are presented in Fig. 2b on the logarithmic scale (the negative values are omitted).

The Minimal Normalized Entropy of the Wavelet Coefficients En

The normalized entropy of the wavelet coefficients of a finite sample is determined by the formula

$$En = -\sum_{k=1}^{N} p_k \log(p_k) / \log(N),$$

$$p_k = c_k^2 \bigg/ \sum_{j=1}^{N} c_j^2, \quad 0 \le En \le 1. \qquad (2)$$

Here, $c_k, k = 1, N$ are the coefficients of orthogonal wavelet expansion with a certain basis. Below, 17 orthogonal Daubechies wavelets are used: ten ordinary bases with the minimal support and one to ten vanishing moments, and seven so-called Daubechies simlets (Mallat, 1998) with four to ten vanishing moments. For each of the bases, the normalized entropy was calculated for the distribution of squared coefficients of (2) and the basis that provides the minimum of (2) was determined. Initially, the minimal value of (2) was considered as a byproduct of the search for the best optimal basis of the orthogonal wavelets. However, later it was noted that this quantity has prognostic properties and its increased values mark the earthquake-prone areas (Lyubushin, 2012b; 2013a; 2013c).

Note that, due to the orthogonality of wavelet transform, the sum of the squared coefficients is equal to the variance (energy) of the signal $X(t)$. Thus, formula (2) calculates the entropy of energy distribution of the oscillations on different spatial and time scales.

Similar to the quantities (1), estimation of *En* was also carried out in the successive windows with a length of one day with preliminary detrending of the data by the polynomials of degree 8. Thus, the time series of the minimal normalized entropy *En*, $0 \le En \le 1$ with a sampling interval of 1 day were obtained for each station.

The Support Width of the Singularity Spectrum $\Delta\alpha$

Consider a certain random oscillation $X(t)$ on the time interval $[[t - \delta/2, t + \delta/2]]$ with a length δ centered at the time point t. Consider the span $\mu(t, \delta)$ of the random oscillation on this interval, i.e., the difference between the maximal and minimal values:

$$\mu(t, \delta) = \max_{t - \delta/2 \le s \le t + \delta/2} X(s) - \min_{t - \delta/2 \le s \le t + \delta/2} X(s). \qquad (3)$$

If $\delta \to 0$, then $\mu(t, \delta)$ also tends to zero; however, here the rate of this decay is important. If the decay is described by the law $\delta^{h(t)}$: $\mu(t, \delta) \underset{\delta \to 0}{\sim} \delta^{h(t)}$ or if there exists the limit $h(t) = \lim_{\delta \to 0} \dfrac{\log(\mu(t, \delta))}{\lg(\delta)}$, the quantity $h(t)$ is referred to as the Helder–Lipschitz exponent. If $h(t)$ is independent of time t: $h(t) = \text{const} = H$, the random oscillation $X(t)$ is referred to as monofractal and H is the Hurst exponent. If the Helder-Lipschitz exponents significantly differ for different time instants t, then, the random oscillation $X(t)$ is multifractal, and the notion of singularity spectrum $F(\alpha)$ can be introduced for it (Feder, 1988). For doing this, we mentally select a set $C(\alpha)$ of such instants of time t that have the same value α of the Helder-Lipschitz constant: $h(t) = \alpha$. The sets $C(\alpha)$ only exist (i.e., contain some elements, are not empty) for certain values of α, that is, there exist some minimal $\alpha_{\min}$ and maximal $\alpha_{\max}$ such that the sets $C(\alpha)$ are not empty only at $\alpha_{\min} < \alpha < \alpha_{\max}$. The multifractal singularity spectrum $F(\alpha)$ is a fractal dimension of the set of the points $C(\alpha)$. Parameter $\Delta\alpha = \alpha_{\max} - \alpha_{\min}$, which is referred to as the support width of the singularity spectrum, is
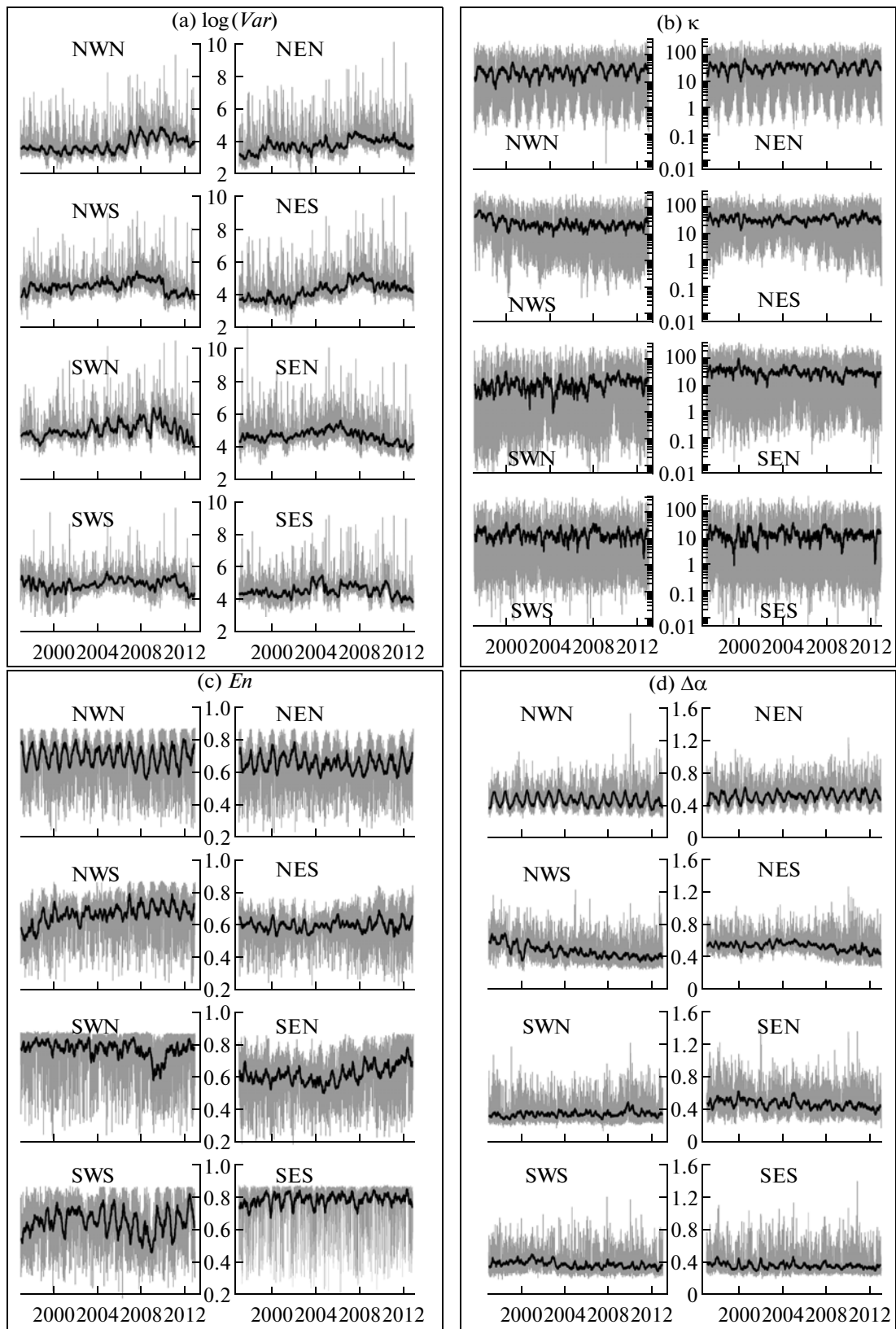
Fig. 2. The gray lines refer to the graphs of daily median values for the four statistics of seismic noise calculated for eight groups of the stations (Fig. 1). The solid black lines refer to the average values in the moving time window with a length of 57 days.
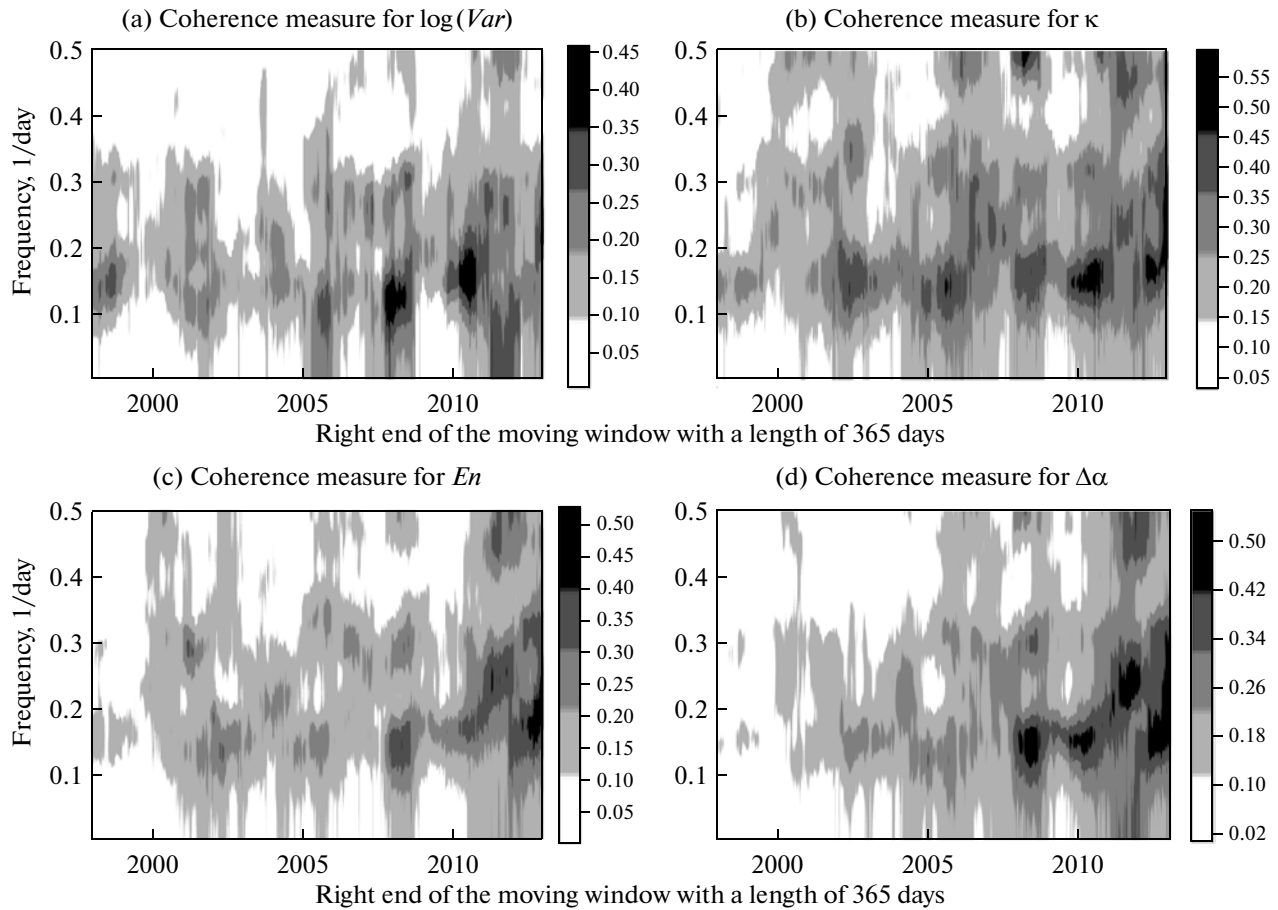
Fig. 3. The frequency-time diagram of variation in the spectral measure of coherence (formula (4)) for the median values of the four statistics of seismic noise from eight groups of the stations (Fig. 2).

perhaps the most important multifractal characteristic and a measure of the diversity in the random behavior of a signal.

Another important characteristic is the argument α^* that conveys the maximum value of the singularity spectrum $F(\alpha^*) = \max\limits_{\alpha_{max} \leq \alpha \leq \alpha_{min}} F(\alpha)$. It is referred to as the generalized Hurst parameter. The maximum of the singularity spectrum cannot exceed unity—the dimension of the embedding set or the time axis: $0 < F(\alpha^*) \leq 1$, typically $F(\alpha^*) = 1$. For a monofractal signal, $\Delta\alpha = 0$ and $\alpha^* = H$. In (Lyubushin and Sobolev, 2006; Lyubushin, 2008), the variations of α^* estimated in the moving time window were used for searching for the coherence in the parameters of seismic noise before the strong earthquakes. In this paper, α^* is not used, because the results of its analysis are qualitatively very similar to the results for $\Delta\alpha$.

The areas of minimal $\Delta\alpha$ trace the earthquake-prone regions, and the statistically significant reduction of the level of $\Delta\alpha$ allowed us to make a conclusion about the incipience of the great Tohoku earthquake of

March 11, 2011 in Japan 2.5 years before the event (Lyubushin, 2009; 2010; 2011a; 2011b; 2012a). The statistics $\Delta\alpha$ and *En* are antipodal and mutually complementary in the dynamical assessment of seismic hazards based on the properties of seismic noise (Lyubushin, 2012; 2013a; 2013c).

The estimation of the multifractal characteristics of seismic noise was carried out for one-minute data in the successive time intervals with a length of 1 day. We used the method that analyzes the fluctuations after elimination of the scale-dependent trends (Kantelhardt et al., 2002). The trends were identified with the use of the local polynomials of order 8. The details of the calculation of the multifractal statistics of the noise are described in (Lyubushin, 2007; 2008; 2009; 2010; 2011a; 2011b) and omitted here.

Thus, just as in the case of the quantities log(*Var*), κ, and *En*, the time series of $\Delta\alpha$ with a time step of 1 day from each station were obtained.

Figure 2 shows the graphs of the daily median values of log(*Var*), κ, *En*, and $\Delta\alpha$ for each of the eight groups of stations (Fig. 1), together with the graphs of
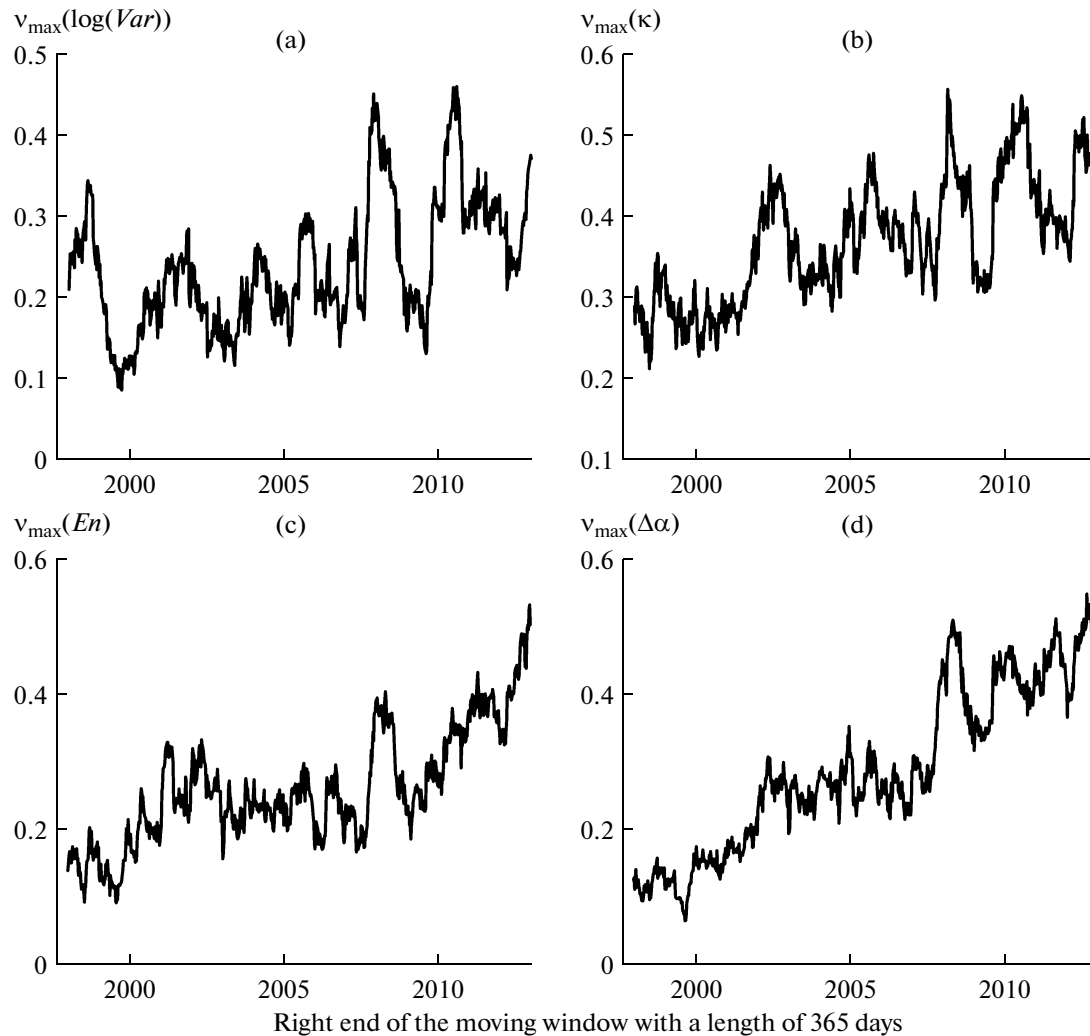
Fig. 4. The maximal (in frequency) values of the spectral measure of coherence (formula 5) calculated for the diagrams in Fig. 3.

their moving averages in the time window of 57 days. The graphs of the averaged values show the clearly pronounced seasonal variations for a few groups of stations, especially for NEN and NWN. Below, we focus on the effects of coherent behavior in the components of four 8-dimensional time series shown in Figs. 2a−2d.
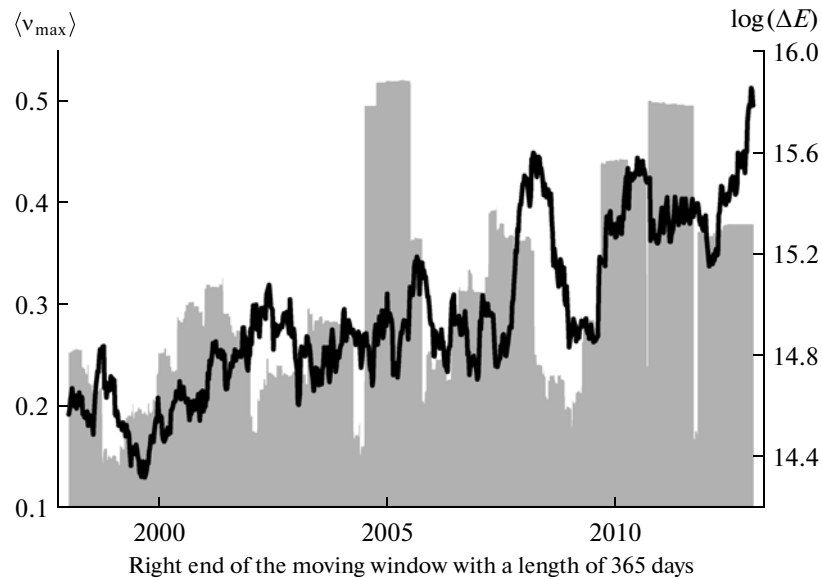
SPECTRAL MEASURE OF COHERENCE

In order to reveal the patterns of synchronous behavior in the average parameters of seismic noise from different groups of stations (Figs. 1 and 2) of the global seismic network, it is suggested to use the spectral measure of coherence (Lyubushin, 1998). Numerous examples of applying this measure in the physics of the solid Earth, hydrology, and climate research are presented in (Lyubushin et al., 2003; 2004; Lyubushin, 2007; 2008; Lyubushin and Sobolev, 2006; Sobolev and Lyubushin, 2007; Lyubushin and Klyashtorin,

2012). The technical details of the computations are described in (Lyubushin, 1998; 2007) and not discussed here. The spectral measure of coherence $\nu(\tau, \omega)$ is determined as the modulus of the product of component-wise multiplication of the canonical coherences

$$\nu(\tau, \omega) = \prod_{j=1}^{m} |\mu_j(\tau, \omega)|. \qquad (4)$$

Here, $m \geq 2$ is the total number of the time series used in the joint analysis (i.e., the dimension of multidimensional time series); ω is frequency; τ is the time coordinate of the right end of the time window containing a certain number of neighboring values (counts); $\mu_j(\tau, \omega)$ is the canonical coherence of the jth scalar time series, which describes the strength of its correlation with the other time series. The quantity $|\mu_j(\tau, \omega)|^2$ is a generalization of the traditional qua-

Fig. 5. The average value of the maximal (in frequency) spectral measures of coherence (formula (6), the black line) against the graph of the logarithmic average of the released seismic energy $\log(\Delta E)$ (J) in the moving time window with a length of 365 days (the gray hatched graph).

dratic spectrum of coherence between two signals for the case when the second signal is a vector instead of scalar. Here, condition $0 \le |\mu_j(\tau,\omega)| \le 1$ is valid, and the closer the value of $|\mu_j(\tau,\omega)|$ to unity, the stronger the linear correlation between the variations in the *j*th time series at frequency ω within the time window with coordinate τ and the similar variations in all the remaining time series. Correspondingly, quantity $\nu(\tau,\omega)$, $0 \le \nu(\tau,\omega) \le 1$, by virtue of its structure, describes the effect of the joint coherent (synchronous, collective) behavior of all signals. Note that, by construction, the value of $\nu(\tau,\omega)$ belongs to the interval [0,1] and the closer the corresponding value to unity, the stronger the linear correlation between the variations in the components of the multidimensional time series at frequency ω in the time window with coordinate τ. It is important that comparison of the absolute values of the statistics $\nu(\tau,\omega)$ is only possible if the number *m* of the time series that are simultaneously used in the processing remains the same, since, due to formula (4), with increasing *m*, the value of ν decreases as a product of *m* values that are less than unity. If only two time series are analyzed, $m = 2$, then function (4) is a conventional quadratic spectrum of coherence (frequency-dependent squared correlation).

In our case, the number of the simultaneously analyzed time series is $m = 8$. For estimating the spectral matrix of multidimensional time series, the vector autoregression model of the fifth order was used (Marple, 1990). The estimation was carried out in the moving time window with a length of 365 days with a mutual shift by 7 days. The selection of the annual

time window was motivated by the necessity to average the effects associated with the seasonal variations in the noise parameters, which are most clearly expressed in Fig. 2 for NEN and NWN groups of stations. It is important that, before calculating the spectral matrix, each scalar component of the multidimensional time series was subjected (independently in each time window) to the following preliminary operations. Primarily, the general linear trend was eliminated and conversion to the increments was carried out. Then, the obtained data were winsorized (Huber, 1981): the sample mean and standard deviation σ were iteratively calculated, the mean was subtracted from the sample, after which the counts were divided by σ and all the values that fell beyond the limits of $\pm 3\sigma$ were replaced by their limiting values. The iterations were repeated until σ stopped changing. These procedures ensure the robustness of the estimate of the coherence measure to the outliers (extreme values).

Besides the frequency–time dependence $\nu(\tau,\omega)$, also the pure time measure of the maximal (over all frequencies) coherence in the current time window with coordinate τ was used:

$$\nu_{max}(\tau) = \max_{\omega} \nu(\tau,\omega). \quad (5)$$

We note that quantity (5) is a certain analog of the coefficient of multiple correlation calculated in the moving time window. However, since the maximum in (5) is taken over the frequencies, this coefficient allows for the time shifts between the scalar components of multidimensional time series within the current time window. Thus, we obtain four maximal measures of coherence as the functions of the time coordinate of the right end of the moving time window:

The strongest earthquakes ($M \geq 8.5$) since beginning of 20th century (according to http://earthquake.usgs.gov/earth-quakes/world/10_largest_world.php)

Date	Magnitude	Latitude	Longitude	Date	Magnitude	Latitude	Longitude
Jan. 31, 1906	8.8	1	−81.5	Mar. 28, 1964	9.2	61.02	−147.65
Nov. 11, 1922	8.5	−28.55	−70.5	Feb. 4, 1965	8.7	51.21	178.5
Feb. 3, 1923	8.5	54	161	Dec. 26, 2004	9.1	3.3	95.78
Feb. 1, 1938	8.5	−5.05	131.62	Mar. 28, 2005	8.6	2.08	97.01
Aug. 15, 1950	8.6	28.5	96.5	Sept. 12, 2007	8.5	−4.438	101.367
Nov. 4, 1952	9.0	52.76	160.06	Feb. 27, 2010	8.8	−35.846	−72.719
Mar. 9, 1957	8.6	51.56	−175.39	Mar. 11, 2011	9.0	38.322	142.369
May 22, 1960	9.5	−38.29	−73.05	Apr. 11, 2012	8.6	2.311	93.063
Oct. 13, 1963	8.5	44.9	149.6				

$\nu_{max}(\tau|\log(Var))$, $\nu_{max}(\tau|\kappa)$, $\nu_{max}(\tau|En)$, and $\nu_{max}(\tau|\Delta\alpha)$, whose graphs are shown in Fig. 4.

We also consider the average of the maximal (in frequency) values of the coherence measures:

$$\langle \nu_{max}(\tau)\rangle = (\nu_{max}(\tau|\log(Var)) \atop + \nu_{max}(\tau|\kappa) + \nu_{max}(\tau|En) + \nu_{max}(\tau|\Delta\alpha))/4. \tag{6}$$

THE RESULTS OF DATA ANALYSIS

The frequency-time diagrams of the spectral measure of coherence (4) for the variations in the studied parameters of seismic noise (Fig. 2) are shown in Fig. 3. The bursts in coherence with increasing amplitudes are observed; the maxima of the bursts fall in the interval of periods of 5 to 10 days. In Fig. 4, which displays the maxima over frequency (5), it can be seen that the average level of synchronization gradually increases, which is particularly well expressed for the multifractal parameter $\Delta\alpha$.

The variations in the average value of the maximal (in frequency) coherence measures (formula (6)) for all the studied parameters are illustrated in Fig. 5. This graph is plotted against the time changes in the logarithmic average of the released seismic energy $\log(\Delta E)$ in the moving time window with a length of 365 days. The graph showing the release of seismic energy is based on the global catalog of seismic events accessible at http://earthquake.usgs.gov/earthquakes/eqarchives/epic.

The comparison of the graphs of $\langle \nu_{max}(\tau)\rangle$ and $\log(\Delta E)$ in Fig. 5 suggests that the correlation between the synchronization levels of seismic noise and the release of seismic energy is non-linear and unambiguous: the burst in the released seismic energy $\log(\Delta E)$ does not necessarily entail the rise in average synchronization (sometimes, even the opposite). The observed variations in the averaged measure of coherence $\langle \nu_{max}(\tau)\rangle$ support the effect of global enhancement of synchronization in seismic noise up to the end of 2012.

The change in the average measures of coherence in Figs. 4 and 5 is not monotonic; it includes a series of local maxima and minima. The question arises, to which extent are these oscillations natural rather than caused by anthropogenic impacts (temporal shutdowns and resumption of functioning of separate seismic stations and putting new stations into operation)? It is worth noting that in order to minimize the anthropogenic effects, the present analysis deals with the median values of the characteristics of noise from each of eight groups of stations, i.e., it handles the most typical values of the statistics from each group of stations, which are robust to the outliers.

CONCLUSIONS

The table summarizes the information on the 17 strongest earthquakes since the beginning of the 20th century. Six of these 17 events occurred within less than ten years starting from the end of 2004. Such earthquakes were absent from February 1965 to the end of 2004, i.e., for almost 40 years.

Thus, it can be hypothesized that the rise of the average level of coherence between the parameters of the global field of seismic noise during the entire period of seismic monitoring from the beginning of 1997 foreran the burst of seismic activity observed since the end of 2004 to present. It is also worth noting that the average level of synchronization was increasing during the entire interval of the observations and at the end of 2012, the average measure of coherence has reached its maximum. The latter can probably be considered as a precursor of the further rise in the intensity of the strongest seismic events, just as it occurred in 1950−1965.

for state support of the leading scientific schools of Russian Federation (grant NSh-5583.2012.5 "Physics and prediction of earthquakes").

REFERENCES

Berger, J., Davis, P., Ekstrom, G., Ambient Earth noise: A survey of the global seismographic network, *J. Geophys. Res.*, 2004, vol. 109, p. B11307.

Feder, J., *Fractals*, New York: Plenum Press, 1988.

Huber, P.J., *Robust Statistics*, New York: Wiley, 1981.

Kantelhardt, J.W., Zschiegner, S.A., Konscienly-Bunde, E., Havlin, S., Bunde, A., and Stanley, H.E., Multifractal detrended fluctuation analysis of nonstationary time series, *Physica A*, 2002, vol. 87, no. 114, pp. 87−114.

Kobayashi, N. and Nishida, K., Continuous excitation of planetary free oscillations by atmospheric disturbances, *Nature*, 1998, vol. 395, pp. 357−360.

Lyubushin, A.A., Analysis of canonical coherences in the problems of geophysical monitoring, *Izv., Phys. Solid Earth*, 1998, vol. 34, no. 1, pp. 52−58.

Lyubushin, A.A., Pisarenko, V.F., Bolgov, M.V., and Rukavishnikova, T.A., The study of general effects in the variations of the river flows, *Meteorol. Gidrol.*, 2003, no. 7, pp. 76−88.

Lyubushin, A.A., Pisarenko, V.F., Bolgov, M.V., Rodkin, M.V., and Rukavishnikova, T.A., Synchronous variations in the Caspian Sea level from coastal observations in 1977−1991, *Izv., Atmos. Oceanic Phys.*, 2004, vol. 40, no. 1, pp. 737−746.

Lyubushin, A.A. and Sobolev, G.A., Multifractal measures of synchronization of microseismic oscillations in a minute range of periods, *Izv., Phys. Solid Earth*, 2006, vol. 42, no. 9, pp. 734−744.

Lyubushin, A.A., *Analiz dannykh sistem geofizicheskogo i ekologicheskogo monitoringa* (Analysis of the Data of Geophysical and Ecological Monitoring), Moscow: Nauka, 2007.

Lyubushin, A.A., Microseismic noise in the low frequency range (periods of 1−300 min): Properties and possible prognostic features, *Izv., Phys. Solid Earth*, 2008, vol. 42, no. 4, pp. 275−290.

Lyubushin, A.A., Synchronization trends and rhythms of multifractal parameters of the field of low-frequency microseisms, *Izv., Phys. Solid Earth*, 2009, vol. 45, no. 5, pp. 381−394.

Lyubushin, A.A., the statistics of the time segments of low-frequency microseisms: trends and synchronization, *Izv., Phys. Solid Earth*, 2010, vol. 46, no. 6, pp. 544−554.

Lyubushin, A.A., Cluster analysis of low-frequency microseismic noise, *Izv., Phys. Solid Earth*, 2011a, vol. 47, no. 6, pp. 488−495.

Lyubushin, A.A., Seismic catastrophe in Japan on March 11, 2011: Long-term forecast based on low-frequency microseisms, *Geofiz. Protsessy Biosfera*, 2011b, vol. 10, no. 1, pp. 9−35.

Lyubushin, A.A. and Klyashtorin, L.B., Short term global *dT* prediction using (60−70)-years periodicity, *Energy Environ.*, 2012, vol. 23, no. 1, pp. 75−85.

Lyubushin, A.A., Forecast of the Great Japan earthquake, *Priroda (*Moscow, Russ. Fed.*)*, 2012a, no. 8, pp. 23−33.

Lyubushin, A., Prognostic properties of low-frequency seismic noise, *Nat. Sci.*, 2012b, vol. 4, no. 8A, pp. 659−666. doi: 10.4236/ns.2012.428087. http://www.scirp.org/journal/PaperInformation.aspx?paperID=21656

Lyubushin, A.A., Mapping the properties of low-frequency microseisms for seismic hazard assessment, *Izv., Phys. Solid Earth*, 2013a, vol. 49, no. 1, pp. 9−18.

Lyubushin, A.A., Maps of linear synchronization for the properties of global low-frequency seismic noise, *Geofiz. Issled.*, 2013b, vol. 14, no. 1, pp. 41−53.

Lyubushin, A.A., Spots of seismic danger extracted by properties of low-frequency seismic noise, *European Geosciences Union General Assembly 2013, Vienna, 7−12 April, 2013, Geophys. Res. Abstracts*, 2013c, Vol. 15, EGU2013-1614. http://meetingorganizer.copernicus.org/EGU2013/EGU2013-1614-1.pdf

Mallat, S., *A Wavelet Tour of Signal Processing*, San Diego: Academic Press, 1998.

Marple, S.L., Jr., *Digital Spectral Analysis with Applications*, Englewood Cliffs, NJ: Prentice-Hall, 1990.

Rhie, J. and Romanowicz, B., Excitation of Earth's continuous free oscillations by atmosphere-ocean-seafloor coupling, *Nature*, 2004, vol. 431, pp. 552−554.

Sobolev, G.A., Microseismic variations prior to a strong earthquake, *Izv., Phys. Solid Earth*, 2004, vol. 40, no. 6, pp. 455−464.

Sobolev, G.A. and Lyubushin, A.A., Microseismic anomalies before the Sumatra earthquake of December 26, 2004, *Izv., Phys. Solid Earth*, 2007, vol. 43, no. 5, pp. 341−353.

Sobolev, G.A., Lyubushin, A.A., Jr., and Zakrzhevskaya, N.A., Synchronization of microseismic variations within a minute range of periods, *Izv., Phys. Solid Earth*, 2005, vol. 41, no. 8, pp. 599−621.

Sobolev, G.A. and Lyubushin, A.A., Microseismic impulses as earthquake precursors, *Izv., Phys. Solid Earth*, 2006, vol. 42, no. 9, pp. 721−733.

Sobolev, G.A., Series of asymmetric pulses in the low-frequency range (periods of 1−300 min) of microseisms as indicators of a metastable state in seismically active zones, *Izv., Phys. Solid Earth*, 2008, vol. 44, no. 4, pp. 261−274.

Sobolev, G.A., A.A. Lyubushin, N.A. Zakrzhevskaya. Asymmetrical pulses, the periodicity and synchronization of low frequency microseisms, *J. Volcanol. Seismol.*, 2008, vol. 2, no. 2, pp. 118−134.

Sobolev, G.A., Low frequency seismic noise before a magnitude 9.0 Tohoku earthquake on March 11, 2011, *Izv., Phys. Solid Earth*, 2011a, vol. 47, no. 12, pp. 1034−1044.

Sobolev, G.A., *Kontseptsiya predskazuemosti zemletryasenii na osnove dinamiki seismichnosti pri triggernom vozdeistvii* (The Concept of Earthquake Predictability Based on the Dynamics of Triggered Seismicity), Moscow: IFZ RAN, 2011b.

Tanimoto, T., The oceanic excitation hypothesis for the continuous oscillations of the Earth, *Geophys. J. Int.*, 2005, vol. 160, pp. 276−288.

Vadzinskii, R.N., *Spravochnik po veroyatnostnym raspredeleniyam* (Reference Book on Probability Distributions), St. Petersburg: Nauka, 2001.

Translated by M. Nazarenko